Stripe Turing structures in a two-dimensional gas discharge system

E. Ammelt,[1,*] Yu. A. Astrov,[1,2] and H.-G. Purwins[1]
[1]*Institute of Applied Physics, University of Münster, Corrensstrasse 2/4, D-48149 Münster, Germany*
[2]*Joffe Physical-Technical Institute of the Russian Academy of Sciences, 194021 St. Petersburg, Russia*
(Received 2 August 1996; revised manuscript received 14 March 1997)

Pattern formation phenomena in current density distributions have been investigated experimentally in a dc-driven planar gas discharge semiconductor system. Patterns are observed and recorded via a light density distribution in the discharge gap, which can be seen through one of the electrodes. Under appropriate conditions the spatially homogeneous discharge glow undertakes a transition into hexagonal or striped patterns as the global current is increased. The observed phenomena are interpreted as a Turing bifurcation into a patterned state. The transition into a striped pattern is studied in detail. Transitions both to stationary and to slowly moving stripe patterns have been observed. It has been ascertained that the typical velocity of stripes, which is of the order of mm/s, is independent of the distance from the bifurcation point in a rather broad range of variation of the bifurcation parameter. The underlying mechanism of pattern formation, as well as the movement of the patterns, is discussed. [S1063-651X(97)11206-5]

PACS number(s): 82.40.Ck, 05.60.+w, 52.80.−s

I. INTRODUCTION

In 1952 Turing [1] proposed a theoretical model for the description of morphogenesis in nature. This principle is still supposed to be basic for the understanding of spatial self-organization in a variety of real systems [2,3]. However, authentic experimental investigations, in which the Turing mechanism is shown to play a decisive role for the creation of diverse spatial patterns, have been published only recently [4–7]. Among the mentioned experimental setups the investigations on Turing patterns in chemical reactions with a disk-shaped active area have become most famous. This may be attributed to their two-dimensional geometry, thus revealing patterns like stripes and hexagons [4,5,8].

In his pioneer work Turing considered diffusion as one of the most important mechanisms to be responsible for the instability of a nonequilibrium state in chemically reacting systems. Nowadays, his model has been applied to systems of quite different origin. This provides the possibility to describe these systems in the frame of the same mathematics as chemical systems, which are destabilized by diffusive transport processes of the reacting substances.

Gas discharge systems generally are essentially nonlinear devices, which can manifest a variety of instabilities [9]. Spatial pattern formation is a widespread phenomenon in these systems. In this context investigations of several two-dimensional dc- and ac-driven systems [10–15] and on a quasi-one-dimensional dc-driven structure [7,16,17] are to be mentioned. Gas discharge systems with layered ''semiconductor-discharge gap'' structures [15], contrary to conventional systems containing metallic electrodes, are of special interest. It was shown earlier that these systems show pattern-forming properties and can be theoretically considered in the frame of the reaction-diffusion mechanism [18,19]. With this approach one was able to comprehend the experimental observations of both spatially regular patterns and solitarylike states (filaments) in these systems [18–21]. In contrast to chemical reactions, in which the transport of material is a basic property, pattern formation phenomena in electronic media are related to the transport of charged carriers and the redistribution of the electric potential. From this point of view electronic media are basically different from chemical or hydrodynamical systems. Nevertheless, phenomena that are similar to those observed in chemical reactors can be found also in electronic devices, in particular in gas discharge systems [14,15]. In contrast to chemical media, in electronic systems spatial structures with small amplitudes are observed less frequently [7]. This fact can be mostly attributed to the strong kind of nonlinearities pertinent to electronic systems. However, under appropriate conditions the nonlinearity can be adjusted in such a way that also soft-mode bifurcations of the Turing type can be observed [7,18]. Up to now the main research on semiconductor-gas discharge systems has been done on quasi-one-dimensional structures [7,16–18]. In [15] we have reported that at the conditions of the cryogenic discharge in nitrogen also two-dimensional regular patterns, hexagons, and stripe structures can be observed experimentally in these media. In the cited publication it was reported how the bifurcation to stationary patterns occurs.

In the present paper we describe results of the further research of pattern formation processes in this system. This experiment provides a very well controlled transition from a narrow linear regime of the discharge to a nonlinear domain, and various kinds of spatial patterns can be observed. On the one hand, we present some scenarios of pattern formation in the system; on the other hand, we give results of the quantitative study of stripe patterns that are known to be among the generic spatial forms appearing in pattern forming systems. Experimental evidence suggests that the formation of a stripe pattern in the considered system usually is accompanied by a slow drift of the pattern. However, also bifurcations into stationary stripe patterns have been verified. In the present work

*FAX: 0049-251-8333513. Electronic address: ammelt@uni-muenster.de

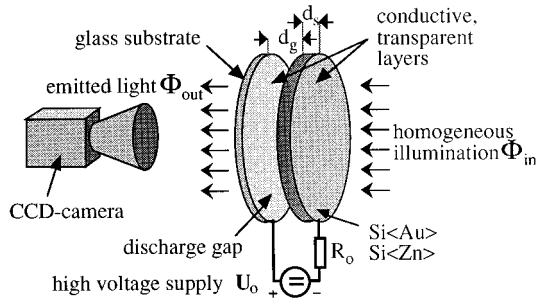

FIG. 1. Experimental setup of the gas discharge system. It consists of two planar electrodes enclosing the discharge gap. The cathode is made of a photosensitive silicon plate and the anode is transparent for the visible light emitted by the discharge. By illuminating the semiconductor its specific resistivity decreases. This may be followed by the destabilization of the spatially homogeneous distribution of the discharge.

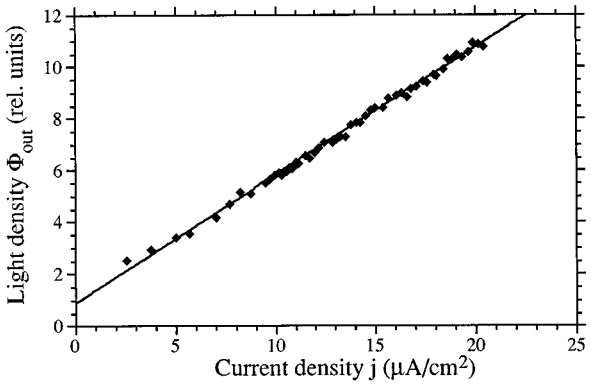

FIG. 2. Mean value of the light density Φ_{out} emitted by the discharge layer as a function of the current density j. As suggested by the linear fit, Φ_{out} is proportional to j in a broad range of the current density. The offset for $j=0$ is due to the electro-optical equipment and has no physical meaning.

the main attention is paid to the defect-free, slowly drifting stripe patterns. Their behavior is compared with the behavior that is specific for stationary patterns.

II. EXPERIMENTAL SETUP

The experiments have been carried out with a planar gas discharge system represented schematically in Fig. 1. The discharge gap is enclosed between a semiconductor cathode and a transparent anode, which is a glass plate covered by an indium-tin-oxide (ITO) layer. As the semiconductor cathode a silicon plate that has been doped with deep impurities of gold or zinc is used. On the external surface the silicon plate carries a transparent, conductive electrode that is prepared either by implantation of B^+ into the semiconductor surface or by evaporation of a thin layer of Ni onto it. The discharge gap is filled with nitrogen at a pressure p in the range 60–200 hPa. Typical values of the thickness of the discharge gap d_g and the silicon plate d_s are $d_g \approx d_s \approx 1$ mm, whereas the diameter of the active region is 20 mm. The dc supply voltage U_0 being applied to the ITO and to the conductive layer on the semiconductor surface ranges from 1.5 to 3.0 kV. A load resistor with $R_0 = 25\ \mathrm{k}\Omega$ is placed in series for current measurement. As the total current usually is less than a few tens of microamperes, the voltage drop across R_0 can be neglected with respect to the supply voltage. The device as a whole is operated close to the liquid-nitrogen temperature ($T \approx 90$ K). By cooling the semiconductor down to this temperature its specific resistivity ρ rises up to $10^7 - 10^9\ \Omega$ m. Taking advantage of the internal photoelectric effect, ρ can be varied by illuminating the semiconductor plate with a tungsten lamp. This experimental arrangement is rather flexible with respect to changes of experimental parameters and scenarios of self-organization processes. Therefore, some of the parameters can be changed interactively.

At low current density the spatially homogeneous distribution of the discharge in the system is stable due to the high resistivity of the semiconductor. By increasing j the discharge passes from the Townsend regime to a range of the charge carrier density in which longitudinal space charges arise, thus entering the nonlinear regime of the discharge layer. Therefore, it is the nonlinearity of the gas layer that is supposed to be responsible for the generation of patterns. Another consequence of the low current density is the rather small power consumption, being in the range $P \leqslant 20\ \mathrm{mW/cm^2}$. During the experimental runs, a variable, homogeneous illumination of the semiconductor has been realized. For the quantitative determination of the illumination density Φ_{in} a silicon photodiode (BPW 544) is installed in the light beam.

According to the model we refer to in a subsequent section, the current density j is the dynamic variable of interest. Since the luminous density Φ_{out} emitted from the discharge gap is related to j, a spatially resolved analysis of j can be carried out. Φ_{out} has been recorded through the transparent ITO anode by a conventional charge coupled device (CCD) camera or a CCD camera with microchannelplate image amplifier, respectively. In both cases the exposure time of $T \leqslant 50$ ms was short compared to the dynamics of the nonstationary patterns we report on below. In order to determine the lateral current density distribution quantitatively, the relationship between Φ_{out} and j should be well known. For this purpose the spatial mean value of Φ_{out} has been measured as a function of the total electric current. As being suggested by the linear fit in Fig. 2, Φ_{out} is proportional to the current density j in a rather good approximation in the parameter range of interest.

III. EXPERIMENTAL RESULTS

The system we investigate shows a rich variety of bifurcation scenarios while varying the experimental parameters. In the following measurements the current density, being controlled by the illumination density, serves exclusively as a bifurcation parameter. Without restrictions, the supply voltage can be used as experimental bifurcation parameter too. The results we present here refer to a particular system with a silicon cathode being heavily doped with Zn at a concentration of up to $2 \times 10^{16}\ \mathrm{cm^{-3}}$. We notice, however, that the same behavior can be found when silicon doped with Au is applied as resistive electrode too.

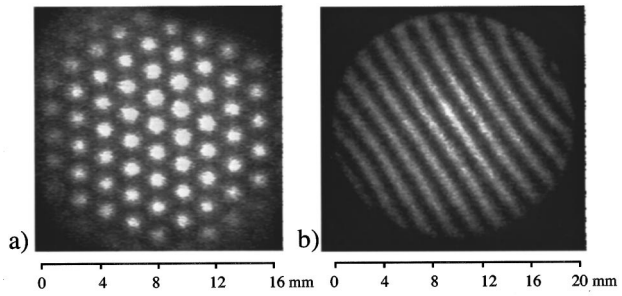

FIG. 3. Density distribution of the emitted glow. Principally two basic kinds of spatial patterns can arise as a result of the instability: (a) a hexagon pattern and (b) a stripe pattern. The parameters are $p=142$ hPa, $d_g=0.80$ mm, and (a) $U_0=1.886$ kV, $j=7.4$ μA/cm^2 and (b) $U_0=2.142$ kV, $j=20.4$ μA/cm^2.

A. Qualitative behavior

For low Φ_{in}, when the resistivity of the semiconductor electrode is high, the increasing of U_0 to a value that exceeds the ignition voltage is accompanied by the appearance of a homogeneous glow in the gap. Starting from this state Φ_{in} is increased gradually, resulting in a homogeneous increase of Φ_{out} until a critical value of Φ_{in} is overstepped. Beyond the threshold value $\Phi_{\text{in}} \geqslant \Phi_{\text{th}}$ a spatially nonhomogeneous distribution of Φ_{out} evolves. Depending on the systems parameters, especially on the gas pressure p and the electrode distance d_g the resulting pattern may be either stationary or nonstationary. In the following our interest focuses on various kinds of stationary or slowly moving patterns. Within the class of stationary structures hexagonal and stripe patterns represent the basic patterns evolving when passing the critical value of the current in the device. In Fig. 3 typical examples for both kinds of patterns are shown. In all cases a further increase of the illumination density leads to nonstationary patterns. This transition is rather independent of the kind of pattern being produced at the first stage of the pattern formation process. Figure 4 shows schematically different cascades of bifurcations we have observed. It is worth mentioning that the stripe pattern may not only develop via the primary bifurcation from the homogeneous state but may also result from the hexagonal pattern in the course of a secondary bifurcation. Results concerning the studies of the hexagonal patterns will be published elsewhere. Here we only notice that both slightly and pronounced subcritical transitions from a homogeneous state to hexagonal patterns can be recorded; the latter occurs predominantly at high pressures. Concerning the stripe pattern, a supercritical transition from the homogeneous state has been observed exclusively.

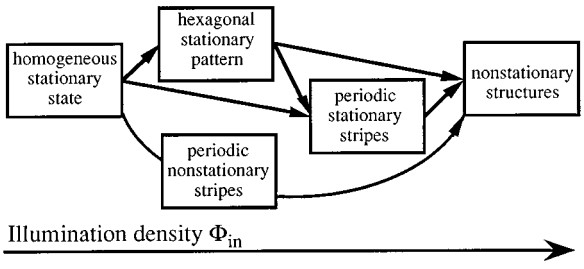

FIG. 4. Observed bifurcation scenarios when varying the illumination density Φ_{in} of the semiconductor cathode. The spatially homogeneous state may be destabilized via different cascades. Depending on the parameters, the initially homogeneous state may be destabilized in favor of a hexagon or a stripe pattern. The hexagon structure may perform a transition to a stripe pattern or to nonstationary structures.

B. Quantitative behavior

In the following the supercritical bifurcation into a periodic stripe pattern is investigated in dependence on the illumination density Φ_{in}. Two gap distances $d_g=0.6$ and 0.8 mm were used in these experiments. The nitrogen pressure in the discharge gap was adjusted in such a way that higher gas pressures were used at lower interelectrode distances. In an experimental run, starting from an established structure, Φ_{in} is decreased gradually far below the bifurcation point while the stripe pattern vanishes steadily. Subsequently, Φ_{in} is increased again and thus the stripe pattern reappears. In this way we are able to register transitions to both stationary and moving patterns. Since the measured velocity v of moving stripes is rather low ($v<1$ mm/s) such patterns are considered to be quasistationary. Although the illumination density Φ_{in} is the experimental controlling parameter, the mean current density j is used as the bifurcation parameter for the following reasons. Accompanying measurements proved that the mean current density depends linearly on the luminous density in a good approximation. From the physical point of view the current density is more characteristic for a discharge system than Φ_{in} and at the same time it is easier to measure. Furthermore, as shown above, the local current density is proportional to the emitted light density. Therefore, the local glow intensity is a good measure for the local current density.

In order to measure the evolving pattern quantitatively, the spatial distribution of the emitted discharge glow has been recorded successively with the camera while varying Φ_{in} gradually. From each image being captured, a rectangular section extending over the entire active region was extracted and processed by a two-dimensional Fourier transformation. In order to diminish the arbitrary influence of the boundaries on the results, the image has been weighted by a ''Hanning'' window previously.

While repeating the experiments at constant external conditions, the system reflects reproducible results in general features. However, some peculiarities in the behavior of the system might be different. For example, for the lowest gas pressures, which was about 60 hPa in the present experiments, we could register moving stripe patterns only. For the intermediate-pressure conditions that we will discuss in the present paper, we could observe transitions of the system either to a stationary or to a moving stripe pattern for some, almost equal conditions. But after evacuating and cooling the system its behavior was reproducible while repeating experimental runs. Having in mind such a behavior of the investigated system, we will present experimental data obtained for transitions both to moving and to stationary patterns, which have been observed at intermediate pressures, and compare them.

1. Bifurcation to a moving stripe pattern

Typical results observed for the transition to moving stripes are represented in Figs. 5–11. In Fig. 5 one-

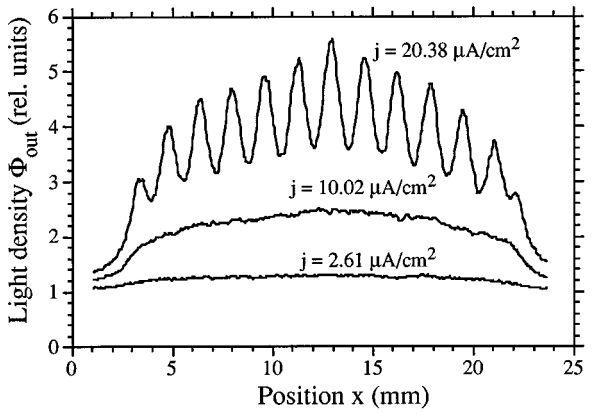

FIG. 5. Light density distributions in the stripe pattern for different values of the control parameter. The parameters are the same as in Fig. 3(b).

dimensional luminous density distributions in the case of the emerging of a stripe pattern are shown for different values of the controlling current density j. The distributions have been measured along the diameter of the discharge plane and perpendicular to the stripe pattern. The initial value of $j = 2.61\ \mu\mathrm{A/cm^2}$ corresponds to some homogeneous state that is specific for low current density. For $j = 10.02\ \mu\mathrm{A/cm^2}$ the distribution reflects the systems state being close to the bifurcation point. At some large value of j ($j = 20.38\ \mu\mathrm{A/cm^2}$) the stripe pattern is fully developed. Notice the spatially decreasing amplitude of the stripe pattern when moving from the center to the boundaries.

Figure 6 shows a linear representation of the contour plot of a section of the two-dimensional amplitude spectrum of the high-amplitude stripe pattern introduced in Fig. 3(b).

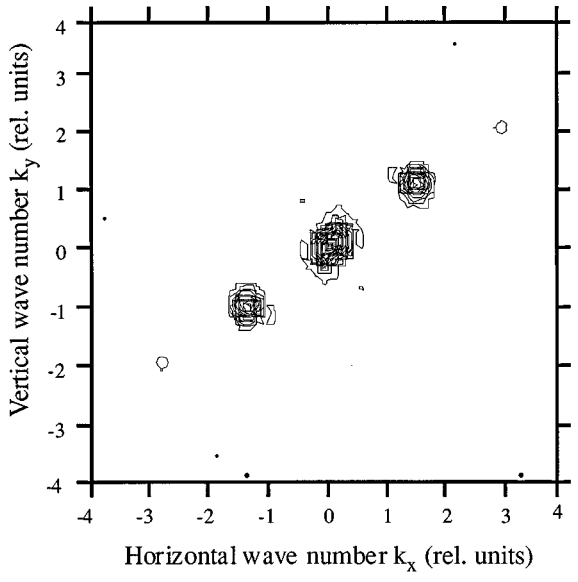

FIG. 6. Contour plot of the two-dimensional amplitude spectrum of the established stripe pattern [Fig. 3(b)]. The central peak corresponds to the spatially homogeneous fraction of the pattern, while the others represent the periodic stripe pattern. As a result of the nonlinear behavior, also the first harmonic rises above the noise level. The parameters are the same as in Fig. 3(b).

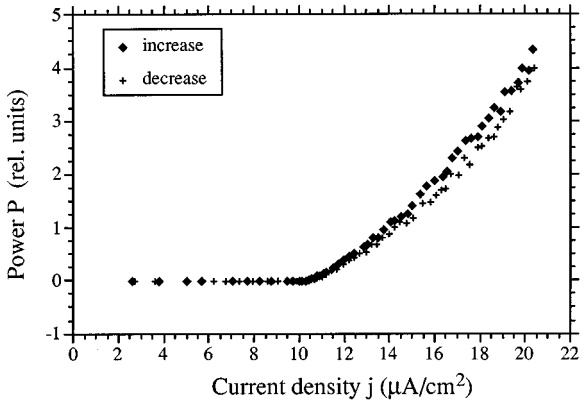

FIG. 7. Power of the leading wave number of a moving stripe pattern for both the increase and decrease control parameter. The pattern evolves when crossing the critical current density. Beyond the bifurcation point the power of the leading wave number smoothly increases as a function of the bifurcation parameter. The parameters are the same as in Fig. 3(b).

Apart from the contribution of the offset at $k = 0$ two peaks appear representing the k value of the periodic stripe pattern. In addition, the first harmonic of the stripe pattern can be noticed. For the quantitative analysis the total power of the leading wave has been calculated by summarizing the spectral power density in the contributing vicinity of the established wave number. This characteristic of the pattern plotted as a function of the mean current density is shown in Fig. 7. Crossing the bifurcation point at $j_c = 10.5 \pm 0.5\ \mu\mathrm{A/cm^2}$, the power increases monotonically with the current. For large values of j a discrepancy between the ascending and the descending curve becomes evident. Within the experimental resolution there was no hysteresis in the vicinity of the bifurcation point. Referring to the curve in Fig. 7, the bifurcation point is not defined very sharply; instead a smooth transition into the rather linear regime can be observed. We also remark that for the conditions represented in Fig. 7, the power of the first harmonic did not exceed 0.5% of that for the leading wave. This indicates that in a broad range of the current the emerging pattern remains rather harmonic.

In the course of this bifurcation the wave number of the evolving stripe pattern varies systematically. Figure 8 shows the wave number as a function of the mean current density. The exact wave number has been determined by calculating the center of mass of the spectral power distribution in the vicinity of the maximum value. In a wide range of the bifurcation parameter the wave number decreases slightly with increasing mean current density.

The error bars shown in Fig. 8 are related to some systematic error of the measuring procedure. They reflect the error of all data points as a whole, whereas the individual errors of the data points are much smaller. Therefore, the data presented in Fig. 8 give evidence for a smooth, continuous variation of k while j changes. In particular the linear fits, shown in the diagram for both upward and downward current changes, suggest a linear and nonhysteretic variation of the wavelength of the pattern as dependent on the control parameter.

The following measurement is devoted to checking whether the spatial orientation of slightly moving stripe pat-

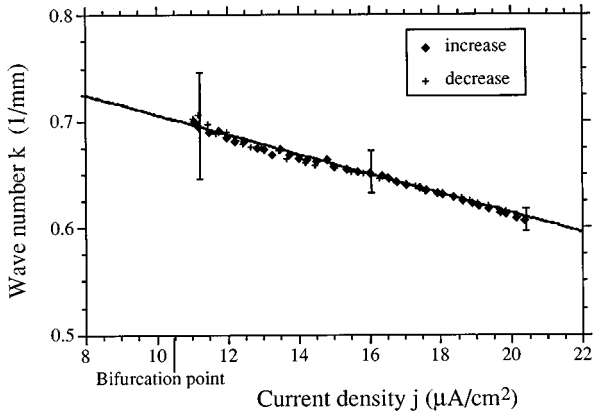

FIG. 8. Wave number of the stripe pattern as a function of the bifurcation parameter. In the course of the bifurcation the wave number of the stripe pattern decreases. Due to the small power of the leading wave number in the vicinity of the bifurcation point the error of the wave number increases drastically. The linear fits for both the increase and decrease of the control parameter reflect some linear dependence. The parameters are the same as in Fig. 3(b).

terns in the plane of the two-dimensional system remains fixed under variation of the bifurcation parameter. As a quantitative measure for the orientation of the pattern the angle of the leading Fourier component against the vertical axis of the experimental system may be chosen. This angle has been determined by calculating the angle of the center of mass of the spectral power density of the related peak. The result is shown in Fig. 9. Although the main direction of the stripe pattern is maintained while the bifurcation parameter changes, a slight rotation of the whole pattern has been revealed. For current densities close to the bifurcation point the scattering of the data points is rather irregular because the total power of the spatial wave is small. At larger values of the mean current density a more systematic behavior exhibiting a hysteresis can be found.

In order to estimate the velocity of the moving stripes as a function of the control parameter the phases of the leading

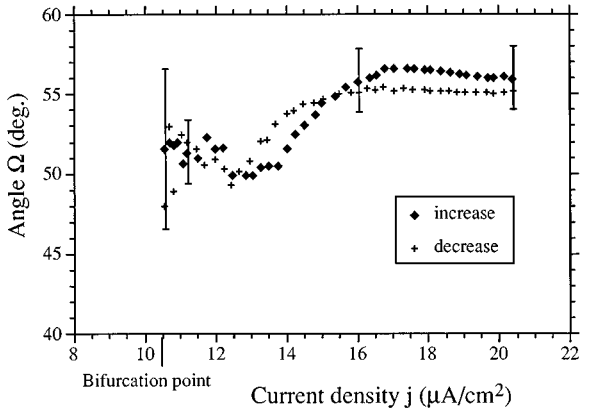

FIG. 9. Orientation Ω of the stripe pattern dependent on the current density. For large values of the bifurcation parameter a systematic deviation of the orientation from that at the bifurcation point can be found as well as a hysteretic behavior of Ω. Close to the bifurcation point the error is rather large. The parameters are the same as in Fig. 3(b).

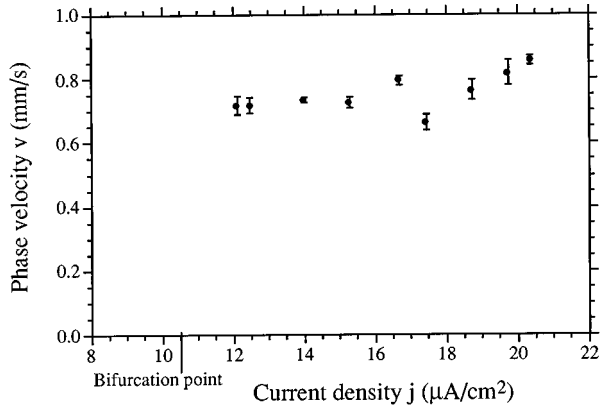

FIG. 10. Phase velocity v of the stripe pattern as a function of the current density in ascending direction. Only a slight variation of the velocity has been observed within the range of change of the bifurcation parameter. The parameters are the same as in Fig. 3(b).

wave number in subsequent images have been compared, thus yielding a value for the phase velocity of the stripe pattern. In Fig. 10 the related data are presented. Obviously, the variation of the velocity is small. Again the precision of the method decreases in the vicinity of the bifurcation point.

Figure 9 shows that at the bifurcation point the pattern moves in quite a definite direction with the velocity $\vec{v}$. This direction can be considered as belonging to some attractor of the system. By increasing the value of the global current the vector $\vec{v}$ is enforced to deviate from the direction that is preferred at the bifurcation point. It is interesting that the number of attractors that control the direction of the movement of the pattern in space may be more than one in this not strictly homogeneous system. In this respect we notice that in addition to the global attractor, some other (higher) attractors that correspond to different spatial orientations of the moving pattern may be adopted by the system. These ''higher'' states can be occupied for some time, but are metastable. The system can be enforced to make a transition from a global attractor into such a ''nonequilibrium'' configuration by some strong perturbation. An example of such a behavior is represented by a set of images, shown in Fig. 11.

Figure 11(a) presents a snapshot of a stripe pattern that is drifting in the direction indicated by the arrow. It is presumed to belong to the global attractor because the pattern does not show any tendency to change the direction of movement during reasonable time of the experiment, say, for some minutes. The system may be strongly perturbed by shadowing some part of the active area of the structure. This is done with a nontransparent mask that is installed in the light beam exciting the semiconductor. In the shadowed domain the current density is strongly suppressed. An example of the system's response to such a perturbation is shown in Fig. 11(b). One can see that the pattern loses its regularity: There is a tendency for stripes to orientate orthogonally to the new internal sharp boundaries. After the mask is removed the system passes through a complicated transient behavior, the characteristic feature of which is the creation of defects, their ''curing,'' and the reconstruction of the whole pattern. For the conditions shown in Fig. 11 such a stage may last as long as several seconds. One of the characteristic appearances of

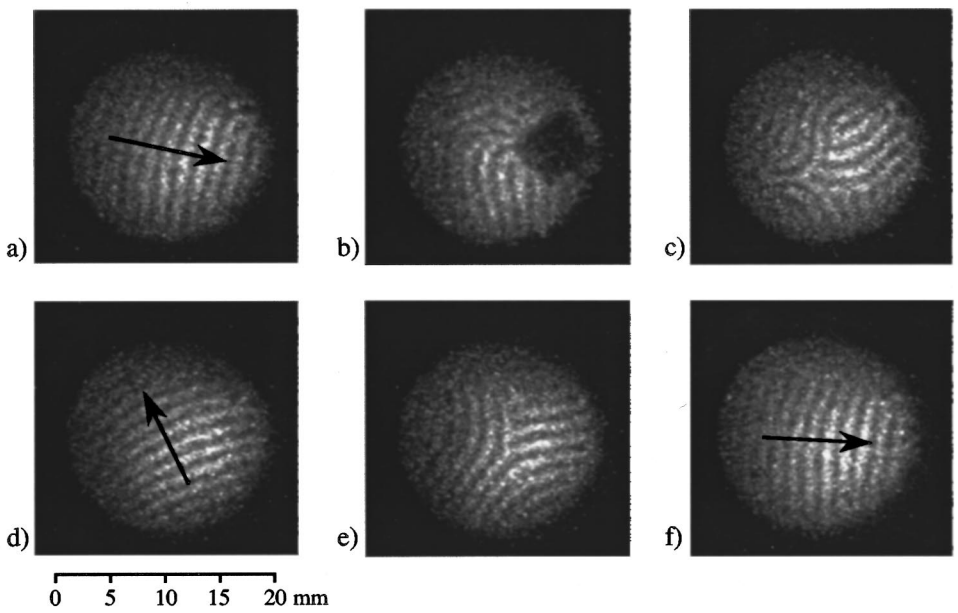

FIG. 11. Appearance of the stripe pattern (a) before, (b) during, and (c)–(f) after some intentional local perturbation of the system. These images show the complex transient behavior of the system while it attempts to comply with the most preferable direction of motion. The observed directions of the steady movement of the pattern are indicated by arrows. The parameters are $p=160$ hPa, $d_g=0.80$ mm, $U_0=2.530$ kV, and $j=9.5$ μA/cm^2.

this behavior is shown in Fig. 11(c). After the relaxation process has finished, the system again finds a striped configuration. It may occur that the regular stripe pattern now drifts in some other direction. This behavior is represented in Fig. 11(d). In this case the new direction does not represent a stable configuration. However, there is a tendency for the system to return to the former configuration, which is represented in Fig. 11(a). To achieve this, a new instability develops being accompanied by the appearance of stripes that propagate in some new direction [Fig. 11(e)]. Finally, the system finds its initial configuration again: The regular stripe pattern moves in the same direction that would be observed before the external perturbation [Fig. 11(f)]. It is worth noticing that in the course of the relaxation of the system to the global attractor, a sequence of attempts to overcome the barrier that separates a higher attractor from the global one may be observed: In the course of such attempts the instability of the kind shown in Fig. 11(e) starts to develop, but then the system may return to the configuration of the Fig. 11(d). At last there may be a successful attempt, and the system passes into a stable final configuration [see Fig. 11(f)], which corresponds to the initial state [Fig. 11(a)].

2. Bifurcation to a stationary stripe pattern

As it was pointed out above, the tendency to form a stationary stripe pattern is more pronounced at higher pressures. It is necessary to have in mind that higher voltages are to be used to feed the system for increased pressure, while other parameters are equal. But applying too-high voltages (in our case $\geqslant 3$ kV) may be not feasible because of the danger of an electrical breakdown of the photoconductor of the system. That is why, from an experimental point of view, while using higher pressures, it is appropriate to diminish the interelectrode distance in the discharge gap, thus keeping the voltage in a reasonable range. In this part of the paper we present experimental data that have been obtained for increased pressure and a diminished value of d_g in comparison to those discussed in the preceding part.

Figure 12 shows the bifurcation curve obtained for the transition of the system from a homogeneous state to a stationary stripe state. When comparing this result with that shown in Fig. 7, one can conclude that the bifurcation behavior is similar to that which has been observed in the case of the slowly moving stripe patterns. It is also worth remarking that the spatial period of the stripe patterns has been diminished by lowering the value of d_g. As in the case of slowly moving stripe patterns, considered above, stationary stripes at the specified experimental conditions also do not

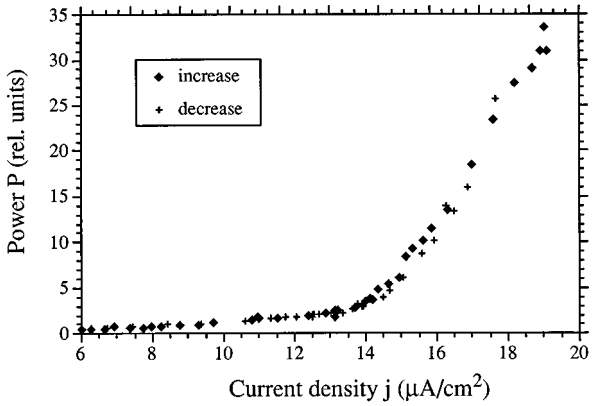

FIG. 12. Power of the leading wave number for both the increase and decrease of the bifurcation parameter for the case of a stationary stripe pattern. At the bifurcation point, a periodic stripe pattern evolves. Beyond the bifurcation point the power of the leading wave number increases monotonically as a function of the bifurcation parameter. The parameters are $p=190$ hPa, $d_g=0.62$ mm, and $U_0=2.750$ kV.

manifest any pronounced nonlinearity in their shape.

However, when comparing the data of Figs. 7 and 12, a somewhat different behavior of the spectra can be observed for low current densities $j < j_c$. The data of Fig. 12 show a continuous increase of the spectral component at the system's leading wave number before the regular pattern appears. This effect is evidently related to the increased influence of spatial inhomogeneities in the discharge area on the distribution of the glow brightness. Nevertheless, the principal features of this transition remain the same as those that have been observed for transitions to the slowly drifting patterns.

As has been mentioned previously, some discrepancy between the ascending and descending branches of the spectral power of the leading wave in the case of moving stripes becomes evident for relatively large values of the bifurcation parameter; see Fig. 7. This behavior is not considered to be typical for this system, neither for moving stripes nor for stationary ones. Instead, the difference between both branches may be attributed to a slight parameter drift, which may occur while the discharge takes place. This parameter drift is assumed to be related to some heating of the semiconductor and complicated processes on the surface of the electrodes that may affect the electric properties of the system rather sensitively. However, these processes are not supposed to be relevant for the pattern formation process we focus on. Therefore, the discrepancy in Fig. 7 is not interpreted in terms of hysteretic behavior. Furthermore, the spectral power function of patterns is shifted for values rather distant from the bifurcation point only, while the critical values of the bifurcation parameter coincide for the case of its increasing and decreasing.

IV. DISCUSSION

One basic experimental feature of the system described here is the supercritical evolution of a periodic stripe pattern. This behavior does not depend on whether the emerging pattern is stationary or slowly drifting in space. In the experiments described, the electric current serves as the bifurcation parameter. The study of the initial state of the system shows that before a bifurcation occurs there exist both smooth radial and smooth angular inhomogeneities in the initial distribution of the current density. The contour plots (Fig. 13) show the light density distribution within a section of the whole active region for a value of the bifurcation parameter slightly below [Fig. 13(a)] and slightly above the bifurcation to the drifting stripe pattern [Fig. 13(b)]. From Fig. 13(a) the global inhomogeneity in the initial current density for the case studied can be evaluated to be in the range $\pm 10-20$ % of the mean value before the bifurcation occurs. As a result, by passing the bifurcation, the critical value is reached at the center first, therefore, the bifurcation does not take place homogeneously. It is worth remarking also that when carefully prepared, the experimental system provides a high homogeneity of the bifurcation parameter over the spatial scale of the order of the pattern's wavelength. This may be the reason why for cases of small spatial gradients in the bifurcation parameter that are observed under these conditions, generally there is no essential pinning effect that could be responsible for the anchoring of the pattern. We also note

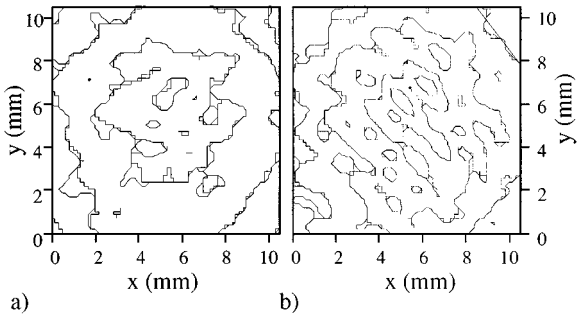

FIG. 13. Contour plot of the light density distribution in a central spatial section for a bifurcation value slightly below ($j = 10.0\ \mu\mathrm{A/cm^2}$, left) and slightly beyond ($j = 10.6\ \mu\mathrm{A/cm^2}$, right) the bifurcation point. The variation of the brightness of the image over the analyzed area as expressed in relative units is from 55 to 75 on the left plot and from 60 to 80 on the right plot. The stepwidth between neighboring lines is 5 each. The parameters are the same as in Fig. 3(b).

the absence of pronounced distortions of the patterns during their drift that could occur as a consequence of these nonhomogeneities. On the other hand, strong localized inhomogeneities in the system can be responsible for the trapping of a pattern or its strong deformation. An example of this is shown in Fig. 14. This picture has been obtained from a pattern that developed when, prior to the start of the experiment, an unintentional contamination of the surfaces of the electrodes had occurred. This had happened due to the condensation of some impurities from the gas-filling system during the cooling of the experimental cell. For these experimental conditions the initial state (not shown) was recorded to contain localized bright spots in the distribution of the discharge glow even at the conditions of the homogeneous illumination of the discharge system.

The regular radial variation of the semiconductor resistivity results from the fact that the semiconductor is cooled only at the boundary, thus leading to a radial variation of the temperature. This is followed by a radial dependence of the

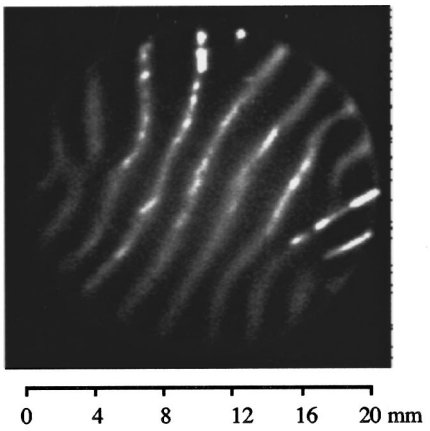

FIG. 14. Example of the stationary stripe pattern in a system with relatively strong localized inhomogeneities. As a result of these unintentional inhomogeneities, the pattern is not strictly periodic and is trapped by inhomogeneities. The parameters are $p = 101$ hPa, $d_g = 1.50$ mm, and (a) $U_0 = 2.50$ kV, $j = 26.2\ \mu\mathrm{A/cm^2}$.

physical parameters of the semiconductor electrode including its sensitivity to the incoming light. Consequently, the resistivity increases radially. Taking into account this inhomogeneous distribution of the resistivity, all the quantitative measurements mentioned above should be carefully considered as the result of a convolution between the spatial parameter distribution and the local system properties. Furthermore, Fig. 13(a) reveals a slight anisotropic orientation of the inhomogeneity in the region of the maximum light density Φ_{out}. Figure 13(b) shows the light density distribution in the same spatial section as in Fig. 13(a) for the slightly developed stripe pattern. Obviously, the pattern evolves just in the region of the maximum of Φ_{out} in Fig. 13(a) and the direction of the pattern is the same as that of the anisotropic central region in Fig. 13(a). Thus the slight intrinsic inhomogeneity of the system provides the ''seed'' for the spatial orientation of the final pattern. The correlation revealed between the geometry of the inhomogeneity of the system and the orientation of the developed pattern is in accordance with the theoretical considerations on systems with ramped conditions [22].

The experimental system has natural boundaries that border the current channel. These borders serve as pronounced inhomogeneities imposed on the system. It is appropriate to recall that the experimental cell we are working with has an aspect ratio, which is the ratio of the diameter of the discharge channel to a period of a pattern, that is rather low.

For bifurcations to stripes the ratio was typically 10–15; see Fig. 3(b). It is surprising that for these conditions a pattern, even if it occupies all the active domain, can drift slowly with a steady velocity, without *jumps* in space. During the movement of the pattern, stripes that are decaying while leaving the active area, as well as incoming stripes that are created on the diametrically opposite side, undertake some deformation, but the core of the pattern moves as a rigid object.

Despite the system's boundaries influence on the periphery of the pattern they seem to undertake no essential effect on the *wave selection* of the emerging and moving pattern because a very smooth dependence of the k value on the control parameter could be registered (see Fig. 8). This suggests that the characteristic wavelength of the pattern is an intrinsic property of the system and is not essentially determined by the presence of the systems boundaries even for the system whose aspect ratio is rather small. However, when diminishing the gap distance in general the wave number of the stripe pattern increases.

In the context of these observations of slowly drifting patterns it is appropriate to consider the internal structure of the current channel inside the experimental cell. The discharge gap extends laterally over a distance of 22 mm in diameter, but close to the physical boundaries of the channel the current density was very low because the diameter of the light beam, which was used to excite the semiconductor, was restricted with a mask of a diameter of 20 mm only (see Fig. 1). As a result, the current density decayed smoothly in the vicinity of the channel boundaries; see Fig. 5. Perhaps this peculiarity of the considered system is among the most important to provide the appearance of moving patterns, even if all the active area is occupied by a pattern.

In contrast to the ''natural'' boundaries of the system, which are rather smooth, some sharper boundaries with arbitrary shape that are located in the central region of the active domain may affect the local behavior of stripes rather strongly; see Fig. 11. The different influence of the system boundaries and some more artificial boundary in the central region, respectively, on spatial pattern formation can be attributed mainly to the following: The system's external boundaries have a rather small curvature and in the case of spatially homogeneous illumination the pattern can accommodate these boundaries without generation of internal defects. (Defects are ''pushed out'' beyond the boundaries.) But when, additionally, some strong perturbation is imposed on the internal area of the pattern, it cannot accommodate both the external and internal boundaries in a defectless manner anymore. As a result, a complex, nonstationary pattern is generated by the system and its movement is accompanied by the complex dynamics of defects inside the pattern.

Mechanism of pattern formation

From the experimental point of view the underlying system evidently consists of two layers, which have quite different properties but are coupled electrically. This provides a starting point for a model description of this system. Various measurements at different parameter values yield that the silicon plate has to be considered as a linear, weakly conductive material, whereas the discharge layer is the nonlinear and therefore the active part of the sandwich structure. Notice that the semiconductor component in this experiment should withstand a voltage drop of greater than or equal to 1 kV in order to operate linearly. Throughout these experiments this demand was met. This concept of the system, being applicable in the present experiment, may not be valid for other discharge arrangements with the same geometrical setup. In particular it is found that a very similar system is stable at a small gap distance of $d_g \approx 100\ \mu$m for a rather large current density of $j \gg 1\ \text{mA/cm}^2$ [23]. For other cases the appearance of lateral pattern formation is related to some instability in the semiconductor cathode, which presumably appears due to the process of charge carrier injection into the high Ohmic semiconductor at a high electric field, while the discharge layer serves as a display medium only [24,25].

In order to understand basic features of spatio temporal pattern formation in electrical systems, a phenomenological model was proposed by Radehaus and co-workers [19,20,26,27]. This model was applied to the description of discrete electrical networks [28] and a quasi-one-dimensional gas discharge system [27]. A basic presupposition of this model is the composition of two layers with different characteristic electrical properties. Although a detailed derivation of the model, the description of its solutions, and its application to a semiconductor-gas discharge structure were published elsewhere [19–21], the basic ideas of this model and its transfer to our experiments are outlined here. One of the layers is assumed to be linear resistive and corresponds to the silicon cathode, whereas the other layer, matching the discharge layer, is characterized by a nonlinear relationship between the voltage drop across this layer and the current density.

The pattern formation in this two layer system can be properly interpreted with a model based on equations of the reaction-diffusion type [18,19]. The physical mechanism that

is incorporated into the model is quite transparent: The nonlinear domain (the gas discharge in the case studied) provides an S-type current density–electric-field characteristic. This behavior is due to the autocatalytic properties of the process of charge carrier multiplication in self-sustained discharges [9]. The gas discharge domain with nonlinear transport properties is responsible for the destabilization of the homogeneous distribution of the current density over the conductive area. Contrary to discharge devices with metallic electrodes, for the system considered here the current density in the narrow discharge gap is controlled by the resistive semiconductor electrode. This linear, spatially distributed load has an inhibiting influence on the electric current density in the gap.

The state of the system and its dynamics were suggested to follow the reaction-diffusion equations [19]

$$\frac{\partial v}{\partial t}=\sigma\Delta v+f(v)-w, \quad \delta\frac{\partial w}{\partial t}=\Delta w+v-w. \tag{1}$$

The variables v and w denote the normalized current density j within the discharge layer and the voltage drop across the semiconductor layer, respectively. Their dynamics are determined by some internal relaxation time constants in the discharge layer and the dielectric properties of the semiconductor expressed in δ as the relative time constant. The Laplace operators take into consideration the lateral diffusion of charge carriers with the relative diffusion constant σ and the lateral spreading of the electric potential in the interface between both layers. Additional terms that take care of the interaction between both components have been derived from the Kirchhoff rules. $f(v)$ symbolizes the normalized, nonlinear current density voltage characteristic of the gas. For appropriate values of the model parameters the homogeneous state can be destabilized in favor of some more complex spatial patterns that can be understood in the framework of local activation and lateral inhibition processes [27].

How does this model explain the bifurcation into periodic stripes? By increasing the density of the cathodes illumination, the conductivity of the semiconductor is increased, resulting in a growth of the discharge current density. Because of this the discharge gradually executes the transition from the Townsend discharge mode to the creation of space charges, thus resulting in a glow discharge state. This process is accompanied by the decrease of the differential slope in the current density-voltage characteristic. At the critical value the negative resistance of the discharge differentially overcompensates the losses in the resistive layer and local activation sets in: Just this destabilization is reflected by the model. Let the slope of $f(v)$ pass a critical value f_c'. Then, under an appropriate choice of the system parameters, the one-dimensional stability analysis yields a supercritical destabilization of the homogeneous state in favor of a periodic wave pattern. The critical wave number k_c is determined by the electric properties and the thickness of both the nonlinear and the linear layer. For the one-dimensional pattern the normalized k_c value can be expressed as [21]

$$k_c=\sqrt{\frac{1}{\sqrt{\sigma}}-1}. \tag{2}$$

As σ is proportional to the inverse of the specific resistivity of the semiconductor ρ the critical wave number k_c is expected to decrease with a decrease of ρ.

This behavior is correlated with the experimental data of Fig. 8. We remark, however, that the perturbation theory, which has been used to obtain the relationship (2), is valid for the bifurcation point exclusively. In the experiment the monotonic decrease of the leading wave number of the pattern is observed in a broad range of current density. The continuous dependence of the pattern period on the distance from the bifurcation point is a rather general phenomenon that has been extensively studied for hydrodynamic systems [2,29,30]. It was theoretically considered in the frame of a weakly nonlinear analysis of pattern formation on planforms in the domain where the harmonic approximation is valid. When the distance from the bifurcation point increases, the number of unstable modes also increases. A stable pattern being formed is controlled by the mechanism of mode selection. At the moment we are not aware of results of a corresponding theoretical analysis of this problem for reaction-diffusion systems. It is worth also adding to the point that the analysis of possible transformations of patterns on a planform, as dependent on the spectral content of growing modes, has revealed other regularities, which are usually graphically presented by the ''Busse balloon'' [29]. It shows domains of stability of modes in k space against instabilities of different symmetries, when the control parameter is changed. Up to now preliminary experimental attempts to observe further pattern transformations described by this theory have not given positive results. When the system is driven further from the domain to which the experimental data of Figs. 7–11 refer, there tends to be a strongly nonstationary behavior of the system. In particular, defects in regular patterns are generated. This process is usually accompanied by the complicated movement of a pattern due to the movement of defects, their recombination, and the creation of new ones.

In addition, for the one-dimensional case, the power of the leading wave number can be calculated by means of the center manifold theory [18,31]. It was found that the power of k_c increases linearly in the vicinity of the bifurcation point when exceeding the critical value. This behavior has been found in this experimental system too; see Fig. 7.

One of the problems raised in the present work is the mechanism of the pattern movement. The intriguing experimental fact is that in a broad range of the control parameter, the velocity of a stripe pattern is constant. This effect, as well as the movement of patterns itself, may be explained in terms of the reaction-diffusion mechanism. The theoretical analysis of this problem shows [32] that inhomogeneities (gradients of parameters) suspend the translational invariance of the system. An inequivalence of different directions in the plane then tries to force the pattern to slide along the active area. It is interesting to point out that if there is a gradient of the diffusion coefficient of at least one of the variables (which is not dependent on the current), then the pattern velocity will not depend on the current value [32]. This is just the case we have observed experimentally (Fig. 10). It seems that a stable and continuous movement can exist in a rather perfect system that contains no strong localized imperfections that could attach a pattern to the electrode surfaces.

V. CONCLUSION

The quasi-two-dimensional electronic (gas discharge) dc-driven system studied shows different scenarios of pattern formation. In the present work these processes have been investigated experimentally with the measurement of the lateral light density distributions emitted by the glow of the discharge. From various spatiotemporal structures being formed, stripe patterns have been discussed in detail. Depending on the parameters, the stripe pattern turns out to be stationary or drifting at a low and constant velocity. The quantitative analysis of the moving stripe pattern shows that the power of the related wave number increases linearly as a function of the bifurcation parameter in a good approximation. Furthermore, the wave number of the established pattern decreases slightly with increasing bifurcation parameter. These experimental results have been discussed in the frame of a quasi-one-dimensional reaction-diffusion model with two components, proposed earlier for electrical two-layer systems. It has been observed that the orientation of the stripe pattern formed in the plane of the gas discharge cell at the bifurcation point is related to an intrinsic inhomogeneity of the system studied. This result is in accordance with theoretical predictions for roll (stripe) patterns in physically ramped systems. However, it has been revealed that under a special strong perturbation the system may undergo transitions to other states with different directions of the movement of the pattern. These states may be occupied for a long time, but are metastable. The system finally relaxes to the initial state, which has to be considered as the global minimum. Finally, this work has demonstrated that the system studied may show quite universal pattern forming behavior with the formation of low-amplitude regular patterns, which has been the subject of research for hydrodynamical and chemical systems for a long time.

ACKNOWLEDGMENTS

We thank M. Bode for his support concerning theoretical questions. This work has been partly supported by the Bundesministerium für Bildung und Forschung (Germany) and by the Russian Academy of Sciences.

[1] A. M. Turing, Philos. Trans. R. Soc. London Ser. B **327**, 37 (1952).
[2] M. C. Cross and P. C. Hohenberg, Rev. Mod. Phys. **65**, 851 (1993).
[3] J. D. Murray, *Mathematical Biology* (Springer, Berlin, 1989).
[4] V. Castets, E. Dulos, J. Boissonade, and P. De Kepper, Phys. Rev. Lett. **64**, 2953 (1990).
[5] Q. Ouyang and H. L. Swinney, Nature **352**, 610 (1991).
[6] H. Willebrand, Diploma treatise, University of Münster, 1988 (unpublished), available from the Institute of Applied Physics, University of Münster, Corrensstrasse 2/4, D-48149 Münster, Germany.
[7] H. Willebrand, C. Radehaus, F.-J. Niedernostheide, R. Dohmen, and H.-G. Purwins, Phys. Lett. A **149**, 131 (1990).
[8] G. H. Gunaratne, Q. Ouyang, and H. L. Swinney, Phys. Rev. E **50**, 2802 (1994).
[9] Y. P. Raizer, *Gas Discharge Physics* (Springer, Berlin, 1991).
[10] D. G. Boyers and W. A. Tiller, J. Appl. Phys. **41**, 28 (1982).
[11] Yu. A. Astrov and L. M. Portsel, Zh. Tekh. Fiz. **51**, 2502 (1981) [Sov. Phys. Tech. Phys. **26**, 1480 (1981)].
[12] E. Ammelt, D. Schweng, and H.-G. Purwins, Phys. Lett. A **179**, 348 (1993).
[13] K.-G. Müller, Phys. Rev. A **37**, 4836 (1988).
[14] W. Breazeal, K. M. Flynn, and E. G. Gwinn, Phys. Rev. E **52**, 1503 (1995).
[15] Yu. Astrov, E. Ammelt, S. Teperick, and H.-G. Purwins, Phys. Lett. A **211**, 184 (1996).
[16] H. Willebrand, F.-J. Niedernostheide, E. Ammelt, R. Dohmen, and H.-G. Purwins, Phys. Lett. A **153**, 437 (1991).
[17] H. Willebrand, F.-J. Niedernostheide, R. Dohmen, and H.-G. Purwins, in *Oscillations and Morphogenesis*, edited by L. Rensing (Dekker, New York, 1992).
[18] C. Radehaus, H. Willebrand, R. Dohmen, F.-J. Niedernostheide, G. Bengel, and H.-G. Purwins, Phys. Rev. A **45**, 2546 (1992).
[19] C. Radehaus, R. Dohmen, H. Willebrand, and F.-J. Niedernostheide, Phys. Rev. A **42**, 7426 (1990).
[20] C. Radehaus, Ph.D. thesis, Münster, 1987 (unpublished), available from the Institute of Applied Physics, University of Münster, Corrensstrasse 2/4, D-48149 Münster, Germany.
[21] R. Dohmen, Ph.D. thesis, Münster, 1991 (unpublished), available from the Institute of Applied Physics, University of Münster, Corrensstrasse 2/4, D-48149 Münster, Germany.
[22] B. A. Malomed and A. A. Nepomnyashchy, Europhys. Lett. **21**, 195 (1993).
[23] Yu. A. Astrov, L. M. Portsel, S. P. Teperick, H. Willebrand, and H.-G. Purwins, J. Appl. Phys. **74**, 2159 (1993).
[24] Yu. A. Astrov, Semiconductors **27**, 1084 (1993).
[25] Yu. A. Astrov and S. A. Khorev, Semiconductors **27**, 1113 (1993).
[26] Ch. Radehaus, K. Kardell, H. Baumann, D. Jäger, and H.-G. Purwins, Z. Phys. B **65**, 515 (1987).
[27] H.-G. Purwins, Ch. Radehaus, T. Dirksmeyer, R. Dohmen, R. Schmeling, and H. Willebrand, Phys. Lett. A **136**, 480 (1989).
[28] H.-G. Purwins, and Ch. Radehaus, in *Pattern Formation on Analogue Parallel Networks*, edited by H. Haken, Springer Series on Synergetics Vol. 42 (Springer, New York, 1988).
[29] F. H. Busse, J. Fluid Mech. **30**, 625 (1967); P. Manneville, *Dissipative Structures and Weak Turbulence* (Academic, New York, 1990).
[30] Y. Hu, R. Ecke, and G. Ahlers, Phys. Rev. E **48**, 4399 (1993).
[31] J. Carr, *Applications of Centre Manifold Theory* (Springer, New York, 1981).
[32] M. Bode (private communication).